

A regularized eigenmatrix method for unstructured sparse recovery

Koung Hee Leem, Jun Liu*, George Pelekanos

Department of Mathematics and Statistics, Southern Illinois University Edwardsville, Edwardsville, IL 62026, USA.

Abstract

The recently developed data-driven eigenmatrix method shows very promising reconstruction accuracy in sparse recovery for a wide range of kernel functions and random sample locations. However, its current implementation can lead to numerical instability if the threshold tolerance is not appropriately chosen. To incorporate regularization techniques, we propose to regularize the eigenmatrix method by replacing the computation of an ill-conditioned pseudo-inverse by the solution of an ill-conditioned least square system, which can be efficiently treated by Tikhonov regularization. Extensive numerical examples confirmed the improved effectiveness of our proposed method, especially when the noise levels are relatively high.

Keywords: Eigenmatrix method, Tikhonov regularization, L-curve rule, ESPRIT algorithm

1. Background

Let X be the parameter space and S be the sampling space. Assume $g(s, x)$ is a given kernel function on $S \times X$ that is analytic in x . Suppose the unknown sparse signal f is given by

$$f(x) = \sum_{k=1}^{n_x} w_k \delta(x - x_k), \quad (1)$$

with δ being the Dirac delta function, and n_x spikes with distinct locations $\{x_k\}$ and weights $\{w_k\}$. The observable for any given sampling point $s \in S$ is given by the following summation

$$u(s) := \int_X g(s, x) f(x) dx = \sum_{k=1}^{n_x} w_k g(s, x_k). \quad (2)$$

Let $\{s_j\}$ be a chosen set of n_s (unstructured) sample locations in S and $u_j = u(s_j)$ be the unknown exact values of observations. In practice, we can only obtain noisy observations, which are assumed to have the following multiplicative form (with an unknown noise magnitude $\sigma > 0$)

$$\tilde{u}_j = u_j (1 + \sigma \mathcal{Z}_j) \quad (3)$$

with \mathcal{Z}_j being independently identically distributed (i.i.d.) standard Gaussian random variables with zero mean and unit variance. Our task is to recover the unknown spike locations $\mathbf{x} := [x_1; x_2; \dots; x_{n_x}]$ and weights $\mathbf{w} := [w_1; w_2; \dots; w_{n_x}]$ from the observation $\{\tilde{u}_j\}$. Obviously, this leads to a highly nonlinear inverse problem that is difficult to treat numerically. The stan-

*Corresponding author.

Email address: juliu@siue.edu (Jun Liu)

standard nonlinear least square formulation will lead to a nonconvex unconstrained optimization problem that can be better solved with a good initial guess estimated by the proposed methods.

Depending on the definition of kernel function g , the sparse recovery problem in the above general form (2) covers a list of well-known sparse recovery problems, such as rational approximation [5], spectral function estimation [22, 23], Fourier inversion [18, 19], Laplace inversion [6, 7, 17, 21], and sparse deconvolution, for which many specially designed numerical algorithms [3, 16] were established with sounding theoretical support in the past few decades; see references in [24]. Nevertheless, these tailored algorithms rely heavily on the underlying structure of each problem, which are not directly applicable to general kernel function with unstructured sampling grid. The developed data-driven eigenmatrix method in [24] does not assume any structures in the kernel function and sampling grid and hence it has a wider applicability than specialized or structured sparse recovery algorithms. Nevertheless, it requires the computation of the pseudo-inverse of a highly ill-conditioned rectangle matrix, which can lead to numerical instability when the threshold tolerance does not match with the underlying noise levels in the measurement data. Our major contribution is to propose a regularized eigenmatrix method that can handle noisy measurement data through modern Tikhonov regularization techniques, which demonstrates significantly improved recovery accuracy in tested numerical examples with high noise levels.

This paper is organized as follows. In Section 2 we briefly review the original eigenmatrix method and point out its drawbacks. In Section 3 we introduce a new regularized eigenmatrix method based on Tikhonov regularization techniques. A few numerical examples are presented in Section 4. Finally, some remarks are concluded in Section 5.

2. Review of the eigenmatrix method

Inspired by the shifting operator defined in the Prony's method and the ESPRIT algorithm [20], the recently developed eigenmatrix method [24] for unstructured sparse recovery problems shows very appealing reconstruction accuracy for different kernels and unstructured sampling locations. Its key idea is to find an n_s -by- n_s eigenmatrix M such that for all $x \in X$ there approximately holds *eigensystem*

$$Mg(x) \approx xg(x), \quad (4)$$

where $g(x) = [g(s_j, x)]_{1 \leq j \leq n_s}$ is an n_s -by-1 vector of functions on X . In numerical implementations, we can enforce this approximate relation over a set of collocation nodes $\{a_t\}_{t=1}^{n_a}$ selected in X . More specifically, if X is the unit disk \mathbb{D} on complex plane, one can select a uniform grid of collocation nodes on the boundary of unit disk, which can be justified by invoking the exponential convergence of trapezoidal rule and the application of Cauchy integral theorem for analytic functions. If X is the real interval $[-1, 1]$, one can choose a Chebyshev grid of collocation nodes on $[-1, 1]$, which can be explained by the Chebyshev quadrature for analytic functions. A general connected domain X can be treated by introducing a smooth one-to-one

map between X and \mathbb{D} or $[-1, 1]$. At this point, there is no error estimates on the accuracy of the approximation (4) in various settings.

Following the notation and methodology introduced in [24], the original eigenmatrix method based on the ESPRIT method mainly consists of the following 4 major steps (not including the postprocessing step for simplicity):

The original eigenmatrix method [24]

- (1) Compute the matrix $G = [g(s_j, a_t)] \in \mathbb{C}^{n_s \times n_a}$ based on the n_s sampling locations $\{s_j\}_{j=1}^{n_s}$ and n_a collocation nodes $\{a_t\}_{t=1}^{n_a}$. Normalize G column-wisely to get \widehat{G} .
- (2) Compute the $n_s \times n_s$ eigenmatrix $M = \widehat{G} \Lambda \widehat{G}^\dagger$, where $\Lambda = \text{diag}(a_t)$ and \widehat{G}^\dagger is the pseudo-inverse of \widehat{G} by thresholding singular values smaller than a given tolerance tol .
- (3) Given the vector of noisy observations \widetilde{u} , choose $l > n_x$ and then compute rank- n_x truncated SVD of the following matrix

$$A := \begin{bmatrix} \widetilde{u} & M\widetilde{u} & \cdots & M^l\widetilde{u} \end{bmatrix} = USV^*. \quad (5)$$

Define V_+^* and V_-^* be the sub-matrix of V^* by deleting the first column and the last column, respectively. The n_x eigenvalues $\{\widetilde{x}_k\}$ of the matrix $V_+^*(V_-^*)^\dagger$ yield the estimated spike locations. Here, we expect (V_-^*) to be well-conditioned.

- (4) With computed $\{\widetilde{x}_k\}$, the weights $\widetilde{w} = [\widetilde{w}_1; \widetilde{w}_2; \cdots; \widetilde{w}_{n_x}]$ can be estimated via a least square problem defined by $\widetilde{G}\widetilde{w} = \widetilde{u}$, where $\widetilde{G} = [g(s_j, \widetilde{x}_k)]$ is of size $n_s \times n_x$.

As a data-driven approach, it involves the key procedure of (approximately) finding the pseudo-inverse \widehat{G}^\dagger of a highly ill-conditioned rectangular matrix \widehat{G} , which was not carefully treated from the perspective of regularization. To alleviate the issue of large condition number, in [24] the author suggested to choose (a small) $n_a = 32$ such that \widehat{G} is of full column rank and its condition number is bounded below by 10^7 . Moreover, the selected thresholding tolerance tol was such that $\|M\|$ is bounded by a small constant such as 3. In their implementations¹ however, the author used $tol = 10^{-4}\|\widehat{G}\|_F$ or $tol = 10^{-8}\|\widehat{G}\|_F$ as the thresholding tolerance in different examples. Hence, the strategy of selecting a small n_a and tol , essentially points to some heuristic regularization treatment, which cannot take into account the actual noise level in the measurements. Therefore, the current version of the eigenmatrix method is less robust in handling a wide range of unknown noise levels.

3. A regularized eigenmatrix method

To make use of modern regularization techniques in the above eigenmatrix method, we need to avoid explicitly computing the ill-conditioned pseudo-inverse matrix \widehat{G}^\dagger . In view of the

¹<https://github.com/lexingying/EigenMatrix>

matrix A in (5), we only need the matrix-vector products $M^k \tilde{\mathbf{u}}$ for $k \geq 1$, which implies that the explicit construction of matrix M is unnecessary. By the theory of pseudo-inverses, if \widehat{G} has **linearly independent columns**, then there holds $\widehat{G}^\dagger \widehat{G} = I_{n_a}$, which leads to

$$M^k \tilde{\mathbf{u}} = (\widehat{G} \Lambda \widehat{G}^\dagger)^k \tilde{\mathbf{u}} = \underbrace{\widehat{G} \Lambda \widehat{G}^\dagger \widehat{G} \Lambda \widehat{G}^\dagger \dots \widehat{G} \Lambda \widehat{G}^\dagger}_{k \text{ times}} \tilde{\mathbf{u}} = \widehat{G} \Lambda^k \widehat{G}^\dagger \tilde{\mathbf{u}}.$$

Let $\mathbf{v} = \widehat{G}^\dagger \tilde{\mathbf{u}}$, then we can rewrite the matrix A in (5) in the form

$$A = \begin{bmatrix} \tilde{\mathbf{u}}, & \widehat{G} \Lambda \mathbf{v}, & \dots, & \widehat{G} \Lambda^l \mathbf{v} \end{bmatrix}. \quad (6)$$

The vector $\mathbf{v} = \widehat{G}^\dagger \tilde{\mathbf{u}}$ can then be obtained from the following ill-conditioned linear system

$$\widehat{G} \mathbf{v} = \tilde{\mathbf{u}} \quad (7)$$

since then we obtain $\mathbf{v} = I_{n_a} \mathbf{v} = \widehat{G}^\dagger (\widehat{G} \mathbf{v}) = \widehat{G}^\dagger \tilde{\mathbf{u}}$. From the above it follows, that there is not even a need to approximately compute the pseudo-inverse \widehat{G}^\dagger or construct the matrix M .

In summary, we propose the following regularized eigenmatrix method without M :

Our proposed regularized eigenmatrix method

- (1) Unchanged.
- (2) Solve the system (7) for \mathbf{v} by Tikhonov regularization method (see below).
- (3) Construct A using (6), and leave the remaining parts unchanged.
- (4) Unchanged.

We reiterate here, that the significant improvement from the original eigenmatrix method is to avoid explicitly computing the eigenmatrix M that requires the computation of the pseudo-inverse \widehat{G}^\dagger . Moreover, the noisy observation $\tilde{\mathbf{u}}$ will influence the computation of \mathbf{v} through the Tikhonov regularization techniques, which do not rely on any manual adjustments of algorithmic parameters.

To demonstrate the role of vector \mathbf{v} in the above method, we consider $\tilde{\mathbf{u}} = \widehat{G} \mathbf{v}$, and we let $\mathbf{a}^k = \text{diag}(\Lambda^k) := [a_1^k; a_2^k; \dots; a_{n_a}^k]$ be a column vector. We then obtain the factorization

$$A = \widehat{G} \begin{bmatrix} \mathbf{v}, & \Lambda \mathbf{v}, & \dots, & \Lambda^l \mathbf{v} \end{bmatrix} = \widehat{G} \text{diag}(\mathbf{v}) [\mathbf{1}, \mathbf{a}, \dots, \mathbf{a}^l], \quad (8)$$

which closely fits the desired factorization structure of the eigenmatrix method, that is

$$A \approx \widetilde{G} \text{diag}(\widetilde{\mathbf{w}}) [\mathbf{1}, \mathbf{x}, \dots, \mathbf{x}^l]. \quad (9)$$

Hence, the entries of the vector \mathbf{v} act as the 'weights' for the corresponding collocation nodes $\{a_t\}$. This connection may be helpful to choose better sampling points $\{s_j\}$ and collocation nodes $\{a_t\}$. For instance, if $n_a = n_x$ such that collocation nodes are identical to the unknown spike locations, we would expect to obtain very accurate reconstruction.

3.1. Tikhonov regularization for solving (7)

We are now ready to employ modern regularization techniques [4, 10, 13, 15] to solve (7). The standard Tikhonov regularization approximates the solution v of (7) by v_γ , which is given as the minimizer of the following Tikhonov regularized objective functional

$$v_\gamma := \arg \min_v \left(\|\widehat{G}v - \widetilde{u}\|^2 + \gamma^2 \|v\|^2 \right), \quad (10)$$

where $\gamma > 0$ is a regularization parameter to be determined. The above Tikhonov minimization problem (10) is mathematically equivalent to solving the regularized normal equation

$$(\widehat{G}^* \widehat{G} + \gamma^2 I)v_\gamma = \widehat{G}^* \widetilde{u}. \quad (11)$$

There are many different a priori or a posteriori methods of choosing a good regularization parameter $\gamma > 0$, such as the Morozov's discrepancy principle [8] that requires the knowledge of noise level. In our numerical experiments, we will apply and compare the established IMPC [2] and L-curve [9, 12] technique² for estimating the regularization parameter γ , since both methods do not require a priori knowledge of the (unknown) noise level in the measured data \widetilde{u} . Both methods yield regularization parameters that are very close to each other, and hence deliver similar reconstruction accuracy. For large-scale problems, computationally more efficient iterative regularization techniques [11, 14] may also be used. Our major contribution is not to develop a new regularization method, but to reformulate the original eigenmatrix method such that the modern regularization techniques can be seamlessly employed.

4. Numerical results

In this section, we will numerically compare the original eigenmatrix method based on pseudo-inverse (denoted by `pinv`) and our proposed regularized eigenmatrix method based on IMPC and L-curve techniques. All simulations are implemented using MATLAB R2024a. To better illustrate the influence of our proposed regularization techniques on the reconstruction accuracy, we will only compare the recovered spike locations and weights based on the ESPRIT algorithm, without the extra postprocessing step of nonlinear optimization that may further improve the accuracy. To measure the reconstruction accuracy, we report the absolute difference of the spike locations and weights separately in Euclidean norm as the overall reconstruction errors, that is

$$\text{errors} = (\|x - \widetilde{x}\|_2, \|w - \widetilde{w}\|_2).$$

We would expect the obtained errors to get smaller as the noise level δ is decreased. We will test the same examples and sampling locations as described in [24], except that the used noise levels are increased by 10 times to better demonstrate the robustness of our proposed regularization

²<http://www2.compute.dtu.dk/~pcha/Regutools/>

techniques. In particular, the spike weights $\{w_k\}$ are set to be one and the noisy observation \tilde{u}_j is constructed by adding different levels of Gaussian noise to the exact observation $u_j = u(s_j)$. The obtained errors are affected by both the used algorithms and the measurement noise, which may show some variance in numerical simulations. To minimize the influence of randomness, we compare all algorithms with the same random noise for a given noise level δ .

4.1. Example 1 (Rational approximation)

In this problem, we have $X = \mathbb{D}$, $g(s, x) = \frac{1}{s-x}$, and true spike locations

$$\boldsymbol{x} = 0.9e^{2\pi i[0.2;0.5;0.8;1]}.$$

We generated $n_s = 40$ random sampling points $\{s_j\}$ outside the unit disk, each with a modulus between 1.2 and 2.2. We then build the matrix $G = [g(s_j, a_t)]$ with $n_a = 32$ uniformly spaced collocation nodes on the unit circle. Figure 1 shows the reconstructed spike locations and weights in comparison with the exact ones by 3 different methods (from top to bottom: pinv, IMPC, and L-curve) with 3 different noise levels. Clearly, our regularized eigenmatrix methods (both IMPC and L-curve) deliver improved recovery (with smaller errors in each column), especially when the noise level gets higher. Both IMPC and L-curve technique yields comparable regularization parameter γ . Notice the threshold tolerance $tol = 10^{-4} \|\widehat{G}\|_F$ used in the original eigenmatrix method is independent of the noise level, which may cause degraded reconstruction accuracy if not appropriately chosen.

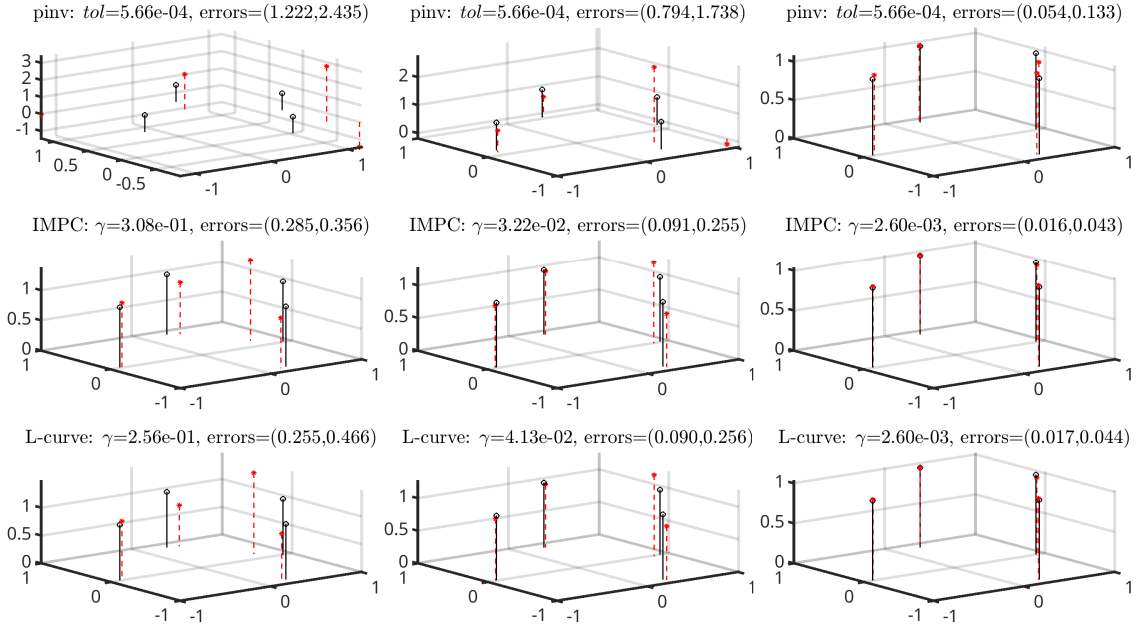


Figure 1: Rational approximation (Columns from left to right: $\sigma = 10^{-1}, 10^{-2}, 10^{-3}$). The exact spikes in solid line and the recovered spikes in dashed line. The errors measure the 2-norm difference in spike locations and weights, respectively.

4.2. Example 2 (Spectral function approximation)

In this problem, we have $X = [-1, 1]$, $g(s, x) = \frac{1}{s-x}$, and true spike locations

$$x = [-0.9; -0.2; 0.2; 0.9].$$

We use $n_s = 256$ uniformly distributed sampling points $s_j = \pm(2j-1)\pi i/\beta, j = 1, 2, \dots, 128$ from the Matsubara grid on the imaginary axis, and then build the matrix $G = [g(s_j, a_t)]$ with $n_a = 32$ Chebyshev collocation nodes on $[-1, 1]$. Figure 2 shows the reconstructed spike locations and weights in comparison with the exact ones by 3 different methods (denoted by pinv, IMPC, and L-curve) with 3 different noise levels. Clearly, our regularized eigenmatrix method (both IMPC and L-curve) delivers more accurate recovery, especially when the noise levels are high.

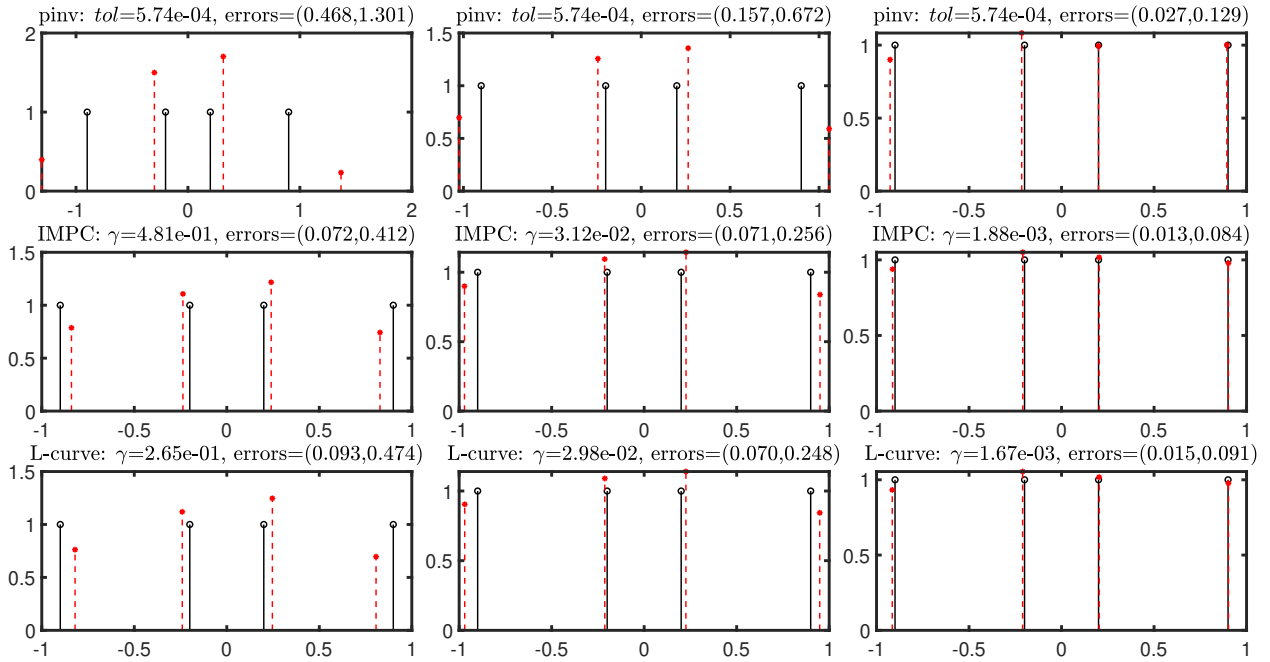


Figure 2: Spectral function approximation (Columns from left to right: $\sigma = 10^{-1}, 10^{-2}, 10^{-3}$). The exact spikes in solid line and the recovered spikes in dashed line. The errors measure the 2-norm difference in spike locations and weights, respectively.

4.3. Example 3 (Fourier inversion)

In this problem, we have $X = [-1, 1]$, $g(s, x) = e^{i\pi s x}$, and true spike locations

$$x = [-0.9; 0; 0.5; 0.9].$$

We generated $n_s = 128$ random sampling points $\{s_j\}$ in $[-5, 5]$, and then build the matrix $G = [g(s_j, a_t)]$ with $n_a = 32$ Chebyshev collocation nodes on $[-1, 1]$. Figure 3 presents the reconstructed spike locations and weights in comparison with the exact ones by 3 different methods

(denoted by pinv, IMPC, and L-curve) with 3 different noise levels. Again, our regularized eigenmatrix method (both IMPC and L-curve) delivers more accurate recovery. It is worthwhile to point out that the original eigenmatrix method also works very well for this problem with small noise levels, likely due to the relatively smaller condition number $\text{cond}(\widehat{G}) \approx 10^7$.

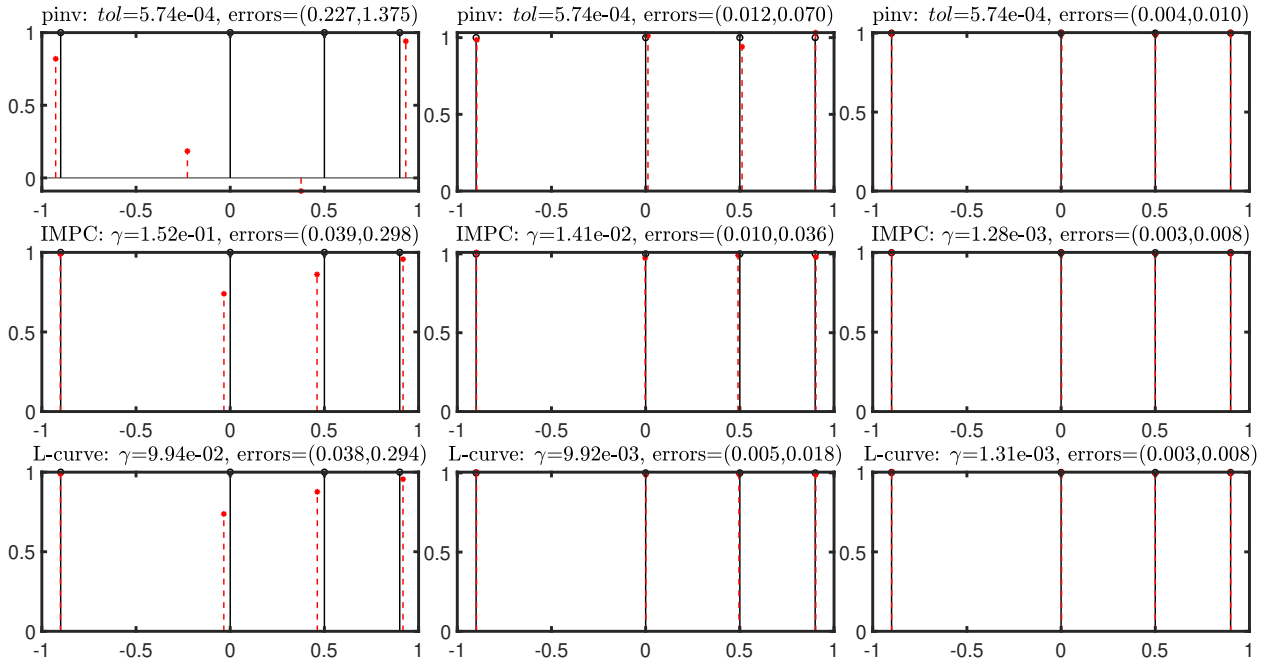


Figure 3: Fourier inversion (Columns from left to right: $\sigma = 10^{-1}, 10^{-2}, 10^{-3}$). The exact spikes in solid line and the recovered spikes in dashed line. The errors measure the 2-norm difference in spike locations and weights, respectively.

4.4. Example 4 (Laplace inversion)

In this problem, we have $X = [0.1, 2.1]$, $g(s, x) = xe^{-sx}$, and true spike locations

$$\mathbf{x} = [0.2; 1.1; 1.6; 2.0].$$

We generated $n_s = 100$ random sampling points $\{s_j\}$ in $[0, 10]$ and then build the matrix $G = [g(s_j, a_t)]$ with $n_a = 32$ shifted Chebyshev collocation nodes on $[0.1, 2.1]$. Notice here \widehat{G} is not of full column rank with $\text{rank}(\widehat{G}) = 17$ and a large condition number $\text{cond}(\widehat{G}) \approx 10^{17}$. In [24] the author only tested very low noise levels ($\sigma = 10^{-5}, 10^{-6}, 10^{-7}$) with a very small threshold tolerance $\text{tol} = 10^{-8} \|\widehat{G}\|_F$, which may conceal the essential difficulty of highly ill-conditioned G . Hence, we will test with higher noise levels ($\sigma = 5 \times 10^{-2}, 5 \times 10^{-3}, 5 \times 10^{-4}$), where we found the moderate threshold tolerance $\text{tol} = 10^{-4} \|\widehat{G}\|_F$ works better in treating higher noise levels.

Figure 4 shows the reconstructed spike locations and weights in comparison with the exact ones by 3 different methods (denoted by pinv, IMPC, and L-curve) with 3 different noise levels. Again, our Tikhonov regularized eigenmatrix method (both IMPC and L-curve) delivers

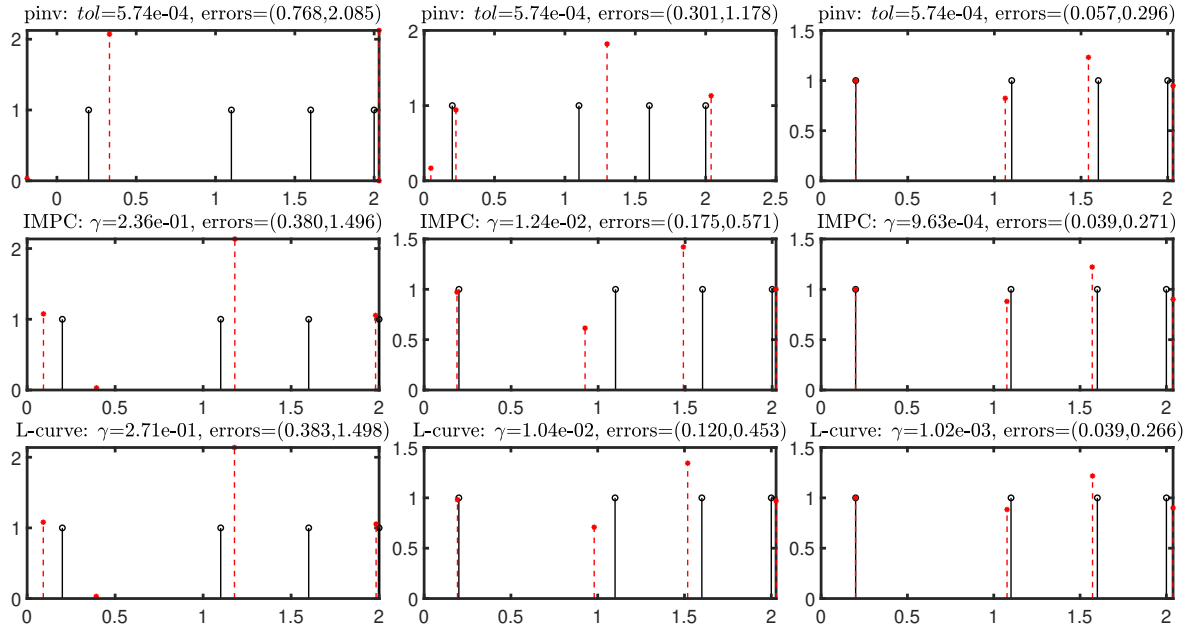


Figure 4: Laplace inversion (Columns from left to right: $2\sigma = 10^{-1}, 10^{-2}, 10^{-3}$). The exact spikes in solid line and the recovered spikes in dashed line. The errors measure the 2-norm difference in spike locations and weights, respectively.

more accurate recovery, which is expected since the most appropriate choice of an threshold tolerance tol requires carefully tuning by hands.

4.5. Example 5 (Sparse deconvolution)

In this problem, we have $X = [-1, 1]$, $g(s, x) = \frac{1}{1+4(s-x)^2}$, and true spike locations

$$\mathbf{x} = [-0.9; 0; 0.5; 0.9].$$

We generated $n_s = 128$ random sampling points $\{s_j\}$ in $[-5, 5]$, and then build the matrix $G = [g(s_j, a_t)]$ with $n_a = 32$ Chebyshev collocation nodes on $[-1, 1]$. Figure 5 displays the reconstructed spike locations and weights in comparison with the exact ones by 3 different methods (denoted by pinv, IMPC, and L-curve) with 3 different noise levels. Again, our Tikhonov regularized eigenmatrix method (both IMPC and L-curve) delivers more accurate recovery.

5. Conclusion

The original eigenmatrix method requires the computation of a pseudo-inverse matrix based on a chosen threshold tolerance, which can not take into account the noise in data. Our proposed regularized eigenmatrix method addressed this shortcoming by incorporating modern regularization techniques, which provide improved recovery as consistently verified by the numerical examples presented above.. The generalization of our approach to multidimensional data recovery [1, 25] is straightforward. For future work, we will be investigating ways to optimize sampling locations.

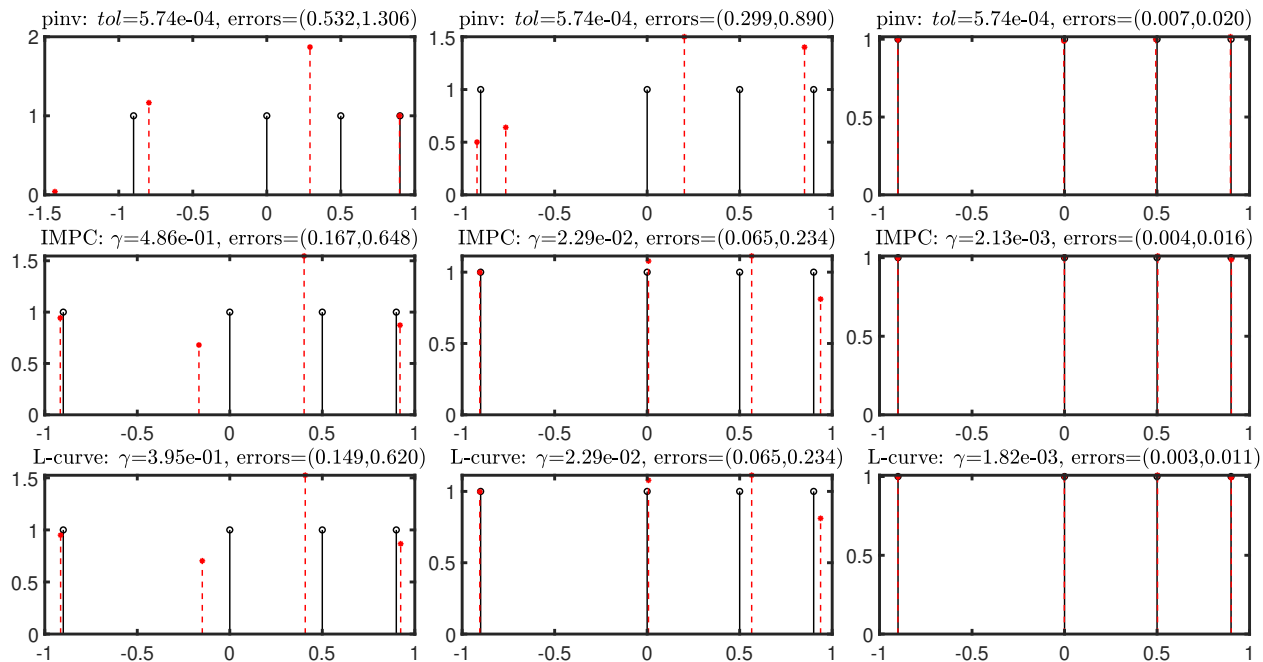


Figure 5: Sparse deconvolution (Columns from left to right: $\sigma = 10^{-1}, 10^{-2}, 10^{-3}$). The exact spikes in solid line and the recovered spikes in dashed line. The errors measure the 2-norm difference in spike locations and weights, respectively.

Declarations

Conflict of interest The authors declare to have no conflict of interests.

References

- [1] F. ANDERSSON AND M. CARLSSON, *ESPRIT for multidimensional general grids*, SIAM Journal on Matrix Analysis and Applications, 39 (2018), pp. 1470–1488.
- [2] F. S. V. BAZÁN AND J. B. FRANCISCO, *An improved fixed-point algorithm for determining a Tikhonov regularization parameter*, Inverse Problems, 25 (2009), p. 045007.
- [3] S. BECKER, J. BOBIN, AND E. J. CANDÈS, *NESTA: A fast and accurate first-order method for sparse recovery*, SIAM Journal on Imaging Sciences, 4 (2011), pp. 1–39.
- [4] M. BENNING AND M. BURGER, *Modern regularization methods for inverse problems*, Acta numerica, 27 (2018), pp. 1–111.
- [5] M. BERLJAJA AND S. GUTTEL, *The RKFIT algorithm for nonlinear rational approximation*, SIAM Journal on Scientific Computing, 39 (2017), pp. A2049–A2071.
- [6] A. COHEN, *Numerical Methods for Laplace Transform Inversion*, Springer US, 2007.
- [7] B. DAVIES AND B. MARTIN, *Numerical inversion of the Laplace transform: a survey and comparison of methods*, Journal of computational physics, 33 (1979), pp. 1–32.

- [8] H. W. ENGL, *Discrepancy principles for Tikhonov regularization of ill-posed problems leading to optimal convergence rates*, Journal of optimization theory and applications, 52 (1987), pp. 209–215.
- [9] H. W. ENGL AND W. GREVER, *Using the L-curve for determining optimal regularization parameters*, Numerische Mathematik, 69 (1994), pp. 25–31.
- [10] H. W. ENGL, M. HANKE, AND A. NEUBAUER, *Regularization of inverse problems*, vol. 375, Springer Science & Business Media, 1996.
- [11] S. GAZZOLA, P. C. HANSEN, AND J. G. NAGY, *IR tools: a MATLAB package of iterative regularization methods and large-scale test problems*, Numerical Algorithms, 81 (2019), pp. 773–811.
- [12] P. C. HANSEN, *Analysis of discrete ill-posed problems by means of the L-curve*, SIAM review, 34 (1992), pp. 561–580.
- [13] —, *Discrete inverse problems: insight and algorithms*, SIAM, 2010.
- [14] P. C. HANSEN AND J. S. JØRGENSEN, *AIR Tools II: algebraic iterative reconstruction methods, improved implementation*, Numerical Algorithms, 79 (2018), pp. 107–137.
- [15] A. KIRSCH, *An Introduction to the Mathematical Theory of Inverse Problems*, Springer New York, 2011.
- [16] E. C. MARQUES, N. MACIEL, L. NAVINER, H. CAI, AND J. YANG, *A review of sparse recovery algorithms*, IEEE access, 7 (2018), pp. 1300–1322.
- [17] T. PETER AND G. PLONKA, *A generalized Prony method for reconstruction of sparse sums of eigenfunctions of linear operators*, Inverse Problems, 29 (2013), p. 025001.
- [18] D. POTTS AND M. TASCHE, *Parameter estimation for exponential sums by approximate Prony method*, Signal Processing, 90 (2010), pp. 1631–1642.
- [19] —, *Parameter estimation for nonincreasing exponential sums by Prony-like methods*, Linear Algebra and its Applications, 439 (2013), pp. 1024–1039.
- [20] R. ROY AND T. KAILATH, *ESPRIT-estimation of signal parameters via rotational invariance techniques*, IEEE Transactions on acoustics, speech, and signal processing, 37 (1989), pp. 984–995.
- [21] W. T. WEEKS, *Numerical inversion of Laplace transforms using Laguerre functions*, Journal of the ACM (JACM), 13 (1966), pp. 419–429.
- [22] L. YING, *Analytic continuation from limited noisy Matsubara data*, Journal of Computational Physics, 469 (2022), p. 111549.
- [23] —, *Pole recovery from noisy data on imaginary axis*, Journal of Scientific Computing, 92 (2022), p. 107.
- [24] —, *Eigenmatrix for unstructured sparse recovery*, Applied and Computational Harmonic Analysis, 71 (2024), p. 101653.
- [25] —, *Multidimensional unstructured sparse recovery via eigenmatrix*, arXiv preprint arXiv:2402.17215, (2024).